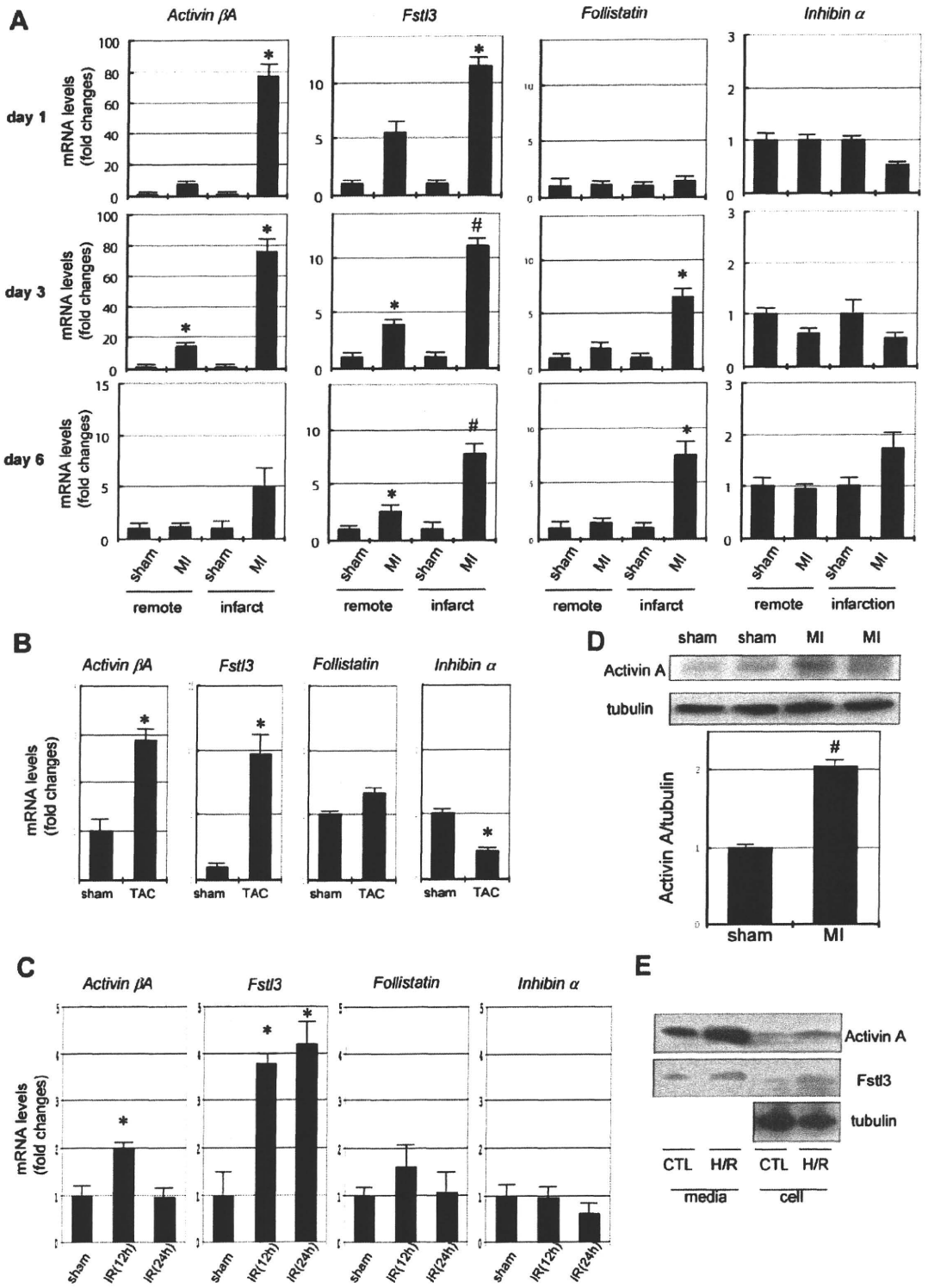

Figure 1. *Fstl3* and *Activin βA* are specifically induced after cardiac injury. Expression analysis of *activin βA*, *Fstl3*, *follistatin*, and *inhibin α* in murine models of myocardial infarction (MI) (A), transverse aortic constriction (TAC) (B), and I/R (IR) (C) is shown. In the myocardial infarction model, samples were taken separately from ischemic zone (infarct area) and nonischemic zone (remote area) 3 days after the onset of myocardial infarction. For the pressure overload model, samples were taken 7 days after transverse aortic constriction surgery. Quantitative real-time polymerase chain reaction was performed to determine the mRNA level of each transcript, and the data were compared with the GAPDH level and normalized to the mean value of controls. n=4 to 6. *$P<0.05$ vs sham; #$P<0.01$ vs sham. D, Upregulation of activin A protein after myocardial infarction. The top panel is a Western blot analysis for activin A performed under nonreducing conditions, and the bottom panel is a blot for α-tubulin with the same samples used under reducing conditions. The histogram shows the quantification of the band intensities for activin A compared with that of tubulin. #$P<0.01$ vs sham. E, Upregulation of activin A and Fstl3 proteins after H/R treatment in NRVM cultures. Representative images of immunoblots of the culture media, 24 hours after addition to cells, and the cell pellet lysates are shown. CTL indicates control.

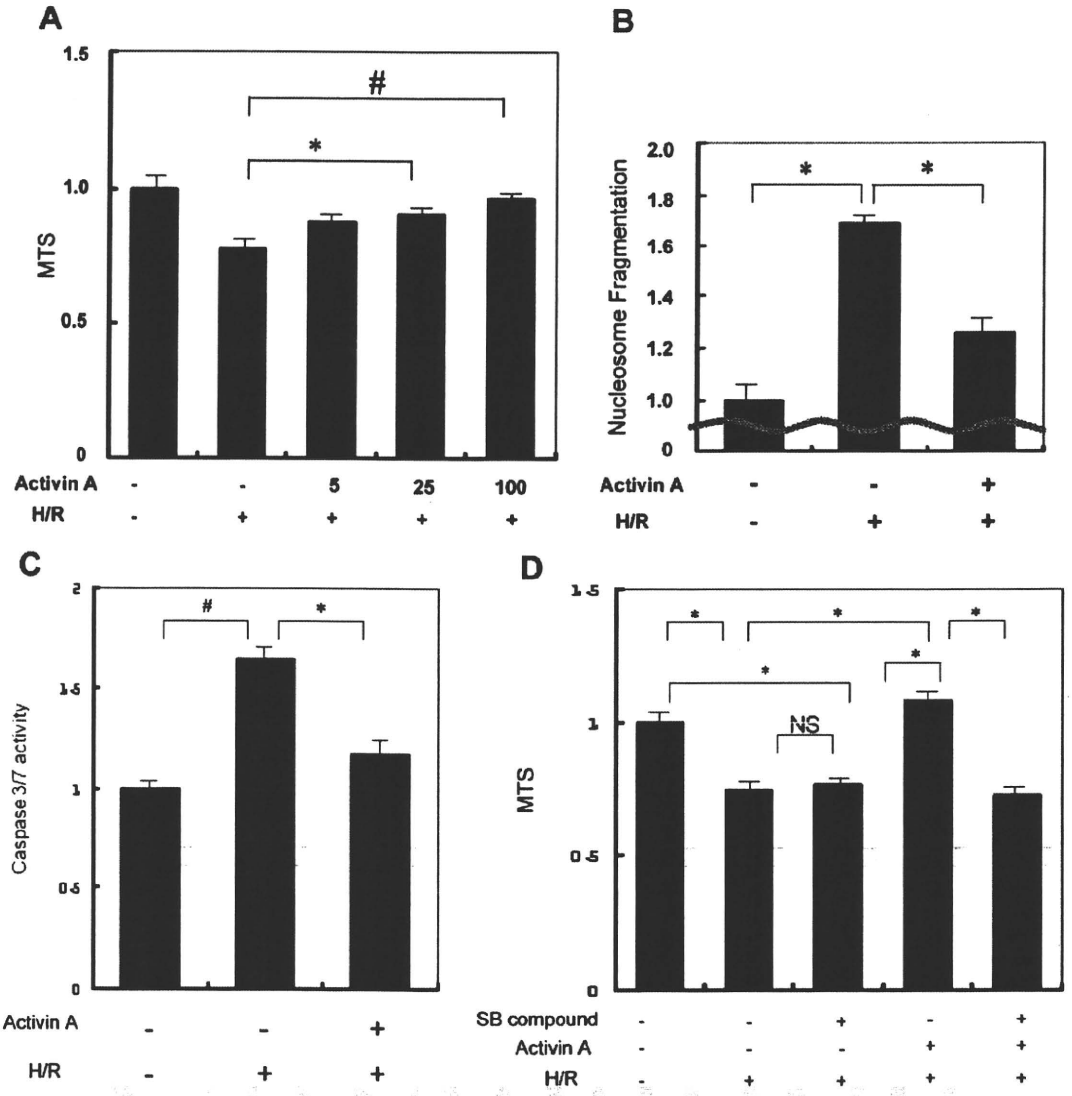

Figure 2. Activin A protects cardiac myocytes from H/R-induced injury. A, NRVMs were pretreated with different concentrations of activin A for 8 hours before the exposure to 12 hours of hypoxia followed by 24 hours of reoxygenation (H/R). Cell viability was determined by the MTS assay. Apoptosis indicated by nucleosome fragmentation assay (B) and caspase-3 and -7 activities (C) were measured in NRVMs pretreated with 25 ng/mL of activin A before exposure to H/R. D, Thirty minutes before addition of activin A, NRVMs were pretreated with or without the inhibitor SB431542 (SB). Cell viability was measured by MTS assay after H/R treatment. *$P<0.05$; #$P<0.01$.

transgene activation,[10] leading us to hypothesize that there might exist as yet unknown networks of autocrine/paracrine factors that control heart function. In this study, we report that cardiac injuries induce the expression of activin A and its binding partner Fstl3. Activin A was found to protect cardiac myocytes from stress-induced cell death, whereas Fstl3 abolished the prosurvival effect of activin A. We propose that activin A and Fstl3 serve as sensors of cardiac stress and that their relative levels of expression influence cell survival in the injured heart.

Methods

See the online-only Data Supplement for additional details.

Myocyte Cultures of Neonatal Rat Ventricular Myocytes

Primary cultures of neonatal rat ventricular myocytes (NRVMs) were incubated in Dulbecco's modified Eagle's medium supplemented with 7% fetal calf serum for 18 to 24 hours after preparation, then with adenoviral vectors at the indicated multiplicity of infection (MOI) for 16 hours in Dulbecco's modified Eagle's medium. The media were then replaced with fresh DMEM without adenovirus and incubated for 12 hours before hypoxia/reoxygenation (H/R). In other experiments, serum-deprived NRVMs were incubated with recombinant activin A protein for 8 hours before H/R. A GasPak system (Becton Dickinson) was used to create hypoxic conditions as described previously.[13] For H/R studies, cells were exposed to 12 hours of hypoxia followed by reoxygenation.

Construction of Adenoviral Vectors Expressing Murine Fstl3 and Murine Activin βA

Full-length *Fstl3* and *activin βA* complementary DNAs (cDNAs) were obtained from American Type Culture Collection. Enzymatic restriction sites were added by polymerase chain reaction on both N- and C-terminus, and the full length of *Fstl3* and *activin βA* and the cDNAs were subcloned into an adenovirus shuttle vector. After linearization, the shuttle vectors were cotransformed into competent

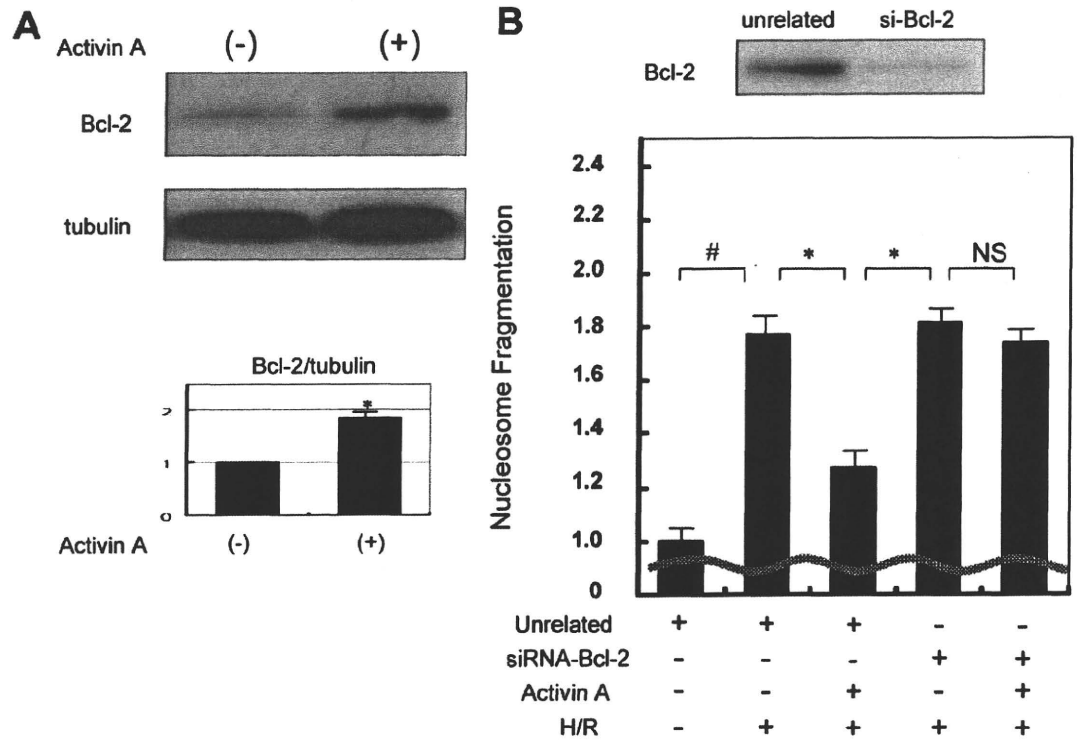

Figure 3. Cytoprotection by activin A is mediated by upregulation of the antiapoptotic protein Bcl-2. A, Activin A–induced Bcl-2 expression in NRVMs. A representative immunoblot is shown. Blots for α-tubulin were performed to indicate the equal loading. The histogram shows quantification of the band intensities to indicate a statistically significant increase in Bcl-2 protein expression after treatment with activin A. *$P<0.05$. B, Ablation of Bcl-2 expression blocks the cytoprotection conferred by activin A. The top panel shows a representative Western blot assessing the efficiency of siRNA targeting Bcl-2. The bottom panel displays the effect of Bcl-2 knockdown on activin A–mediated cytoprotection of NRVMs as determined by nucleosome fragmentation assay. Apoptosis was induced by H/R treatment. *$P<0.05$; #$P<0.01$.

cells (TOP10; Invitrogen) with the adenoviral backbone plasmid (pAdEasy-1). The recombinant adenoviral DNA with *Fstl3* or *activin βA* cDNA was extracted from the competent cells and transfected into HEK 293 cells to produce recombinant adenoviral vectors that express *Fstl3* (Ad-Fstl3) or *activin βA* (Ad-actβA). An adenoviral vector expressing β-galactosidase (Ad-βgal) was used as a control. The adenoviral vectors were purified by the CsCl ultracentrifugation method.

Adenovirus-Mediated Overexpression of Activin A in Mice

Eight- to 10-week-old male mice were injected intravenously with adenovirus (Ad-actβA or Ad-βgal; 5.0×10^9 plaque-forming units per mouse) through the jugular vein. Plasma activin A was assayed by Western blot analysis 3 days after adenovirus delivery. At this time point, mice also underwent myocardial ischemia/reperfusion (I/R) injury.

Generation of a Cardiac-Specific *Fstl3* Knockout Mice

Mice homozygous for an *Fstl3* allele with 2 *lox*P sites flanking exons 3 through 5 ($Fstl3^{flox/flox}$) were backcrossed and maintained on the C57BL6/J background. $Fstl3^{flox/flox}$ were crossed with α-myosin heavy chain (α-MHC)-Cre transgenic mice that are maintained on a C57BL6/J background. Four different primer pairs were used for genotyping polymerase chain reaction. The *lox*P site in intron 2 was detected with the use of the primer 1 (SJL954 TCTGAGAAGAG-GAGGGATTTCAAG) and primer 2 (SJL955 ATTTACACCTAGC-CACATACTCTG), which amplify an ≈390-bp fragment for the *lox*P site, whereas the *Fstl3* wild-type allele gives a 330-bp fragment. The *lox*P site in intron 5 was detected with the use of primer 3 (SJL956 AACCACATCCCAGATCCAGGTCAC) and primer 4 (SJL986 CAGCTATGTAGGCTTTGCATTGCTC), which amplify an ≈310-bp fragment for the *lox*P site and a 270-bp fragment for the wild-type allele. Recombination by Cre leads to an allele that lacks exons 3, 4, and 5 of the *Fstl3* gene and is detected with the use of primer pair of 1 and 4, which gives a 357-bp fragment. The α-MHC-Cre transgene is detected with the use of the primer pair of 5′-ATGACAGACAGATCCCTCCTATCTCC and 5′-CTCATCAC-TCGTTGCATCATCGAC, which amplifies a 300-bp fragment.

Statistical Analysis

Data are presented as mean±SEM. Group differences were analyzed by 2-tailed Student *t* test or ANOVA. To compare multiple groups, the Mann–Whitney *U* test with Bonferroni correction was used. A value of $P<0.05$ was considered statistically significant.

The authors had full access to and take full responsibility for the integrity of the data. All authors have read and agree to the manuscript as written.

Results

Activin βA and *Fstl3* Levels Are Regulated by Stress in the Heart

To better understand the roles of the TGF-β superfamily cytokines in heart, we analyzed transcript expression of family members by quantitative real-time polymerase chain reaction using cDNAs from mouse heart (Figure 1A). These analyses focused on *activin βA*, its inhibitory binding partners *follistatin* and *Fstl3*, and *inhibin α*. *Activin βA* showed marked upregulation at 1 and 3 days after left coronary artery

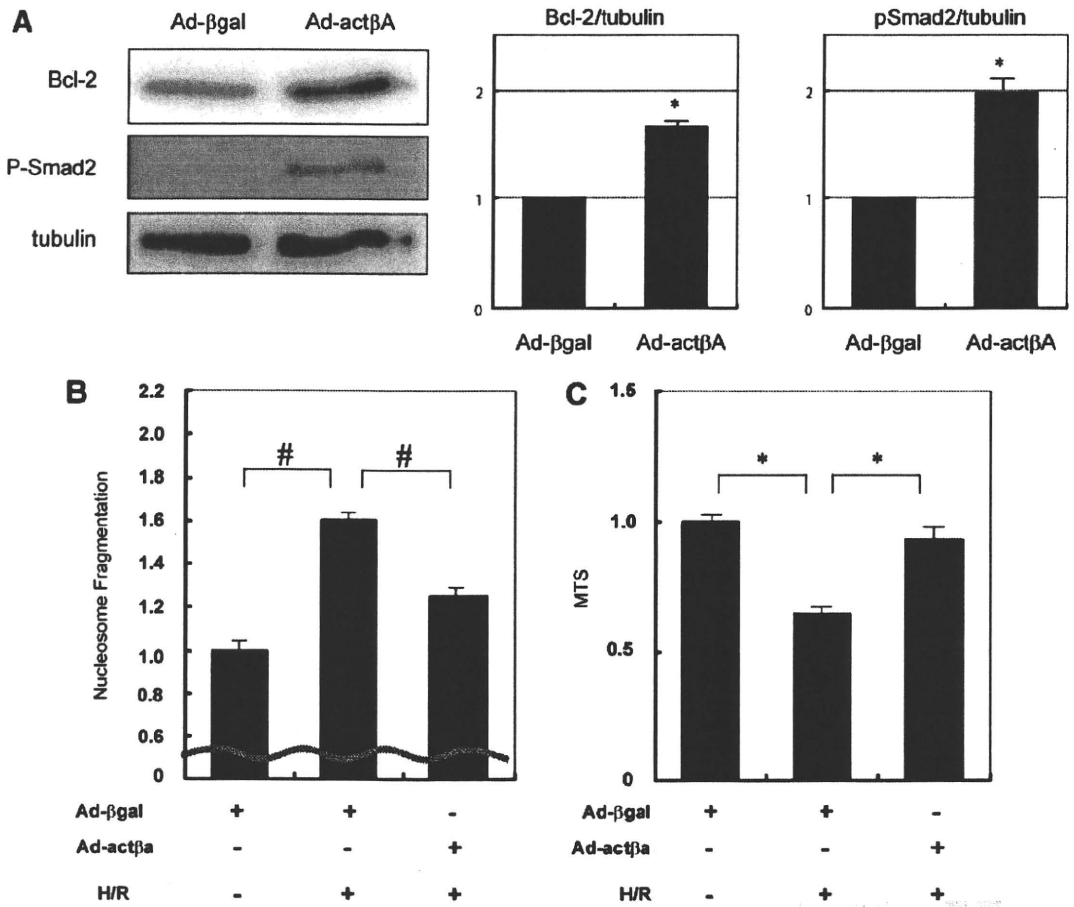

Figure 4. Adenovirus-encoded activin A induces Bcl-2 and protects cardiac myocytes from stress. A, Representative immunoblot images showing that transfection of adenoviral vector expressing *activin βA* (Ad-actβA) at an MOI of 50 resulted in increased expression of Bcl-2 and phosphorylation of Smad2. Membranes were blotted for α-tubulin to indicate equal protein loading. Histogram shows quantification of the band intensities. *$P<0.05$. Transduction of Ad-actβA (MOI=50) reduced apoptosis, assessed by the nucleosome fragmentation assay (B), and preserved cell viability, assessed by the MTS assay (C), against H/R stress. An adenovirus vector expressing β-galactosidase (Ad-βgal) was used as a control in these experiments at an MOI of 50. *$P<0.05$; #$P<0.01$.

ligation in the infarct zone and returned to baseline at the 6-day time point. These findings are in general agreement with those of Yndestad et al,[14] who previously reported a 15- to 40-fold induction of *activin βA* in the ischemic regions of heart after left coronary artery ligation in rats. *Fstl3* displayed statistically significant upregulation at days 1, 3, and 6 in the infarct and remote regions after left coronary artery ligation. *Follistatin* upregulation was observed in the infarct zone at the 3- and 6-day time points. No regulation of *inhibin* α, which opposes the action of *activin A*, was observed in this model.

Activin βA and *Fstl3* were upregulated 10- and 3-fold, respectively, after pressure overload at 1 week after transverse aortic constriction (Figure 1B), whereas the *follistatin* transcript level did not change, and the *inhibin* α transcript level declined by a factor of 2 (Figure 1B). In an I/R model, *Fstl3* expression was upregulated 4-fold at 12- and 24-hour time points after perfusion, whereas levels of *activin βA* increased 2-fold at the 12-hour time point (Figure 1C). Levels of *follistatin* and *inhibin* α did not change in these assays.

Dimers of activin βA are processed to give rise to the physiologically active protein activin A. Activin A levels were measured in hearts 3 days after left coronary artery ligation because the *activin βA* transcript was expressed robustly at this time point. A significant increase in activin A protein could be detected in hearts after infarction (Figure 1D). To document activin A and Fstl3 expression by cardiac myocytes, NRVMs were cultured under normoxic and H/R conditions (Figure 1E). Both proteins could be detected in lysates of the cell pellets and in the conditioned media. Treatment of cultures by H/R led to a 1.9-fold upregulation of activin A and a 1.7-fold upregulation of Fstl3 in the culture media ($P<0.05$; n=6).

Activin A Protects Cultured Myocytes From Apoptosis

In the noncardiac cell type, activin A has been reported to promote survival[15–17] or apoptosis.[18,19] Thus far, the effects of activin A on cardiac myocyte survival have not been reported. To elucidate the functional significance of activin A in cardiac myocytes, serum-deprived NRVMs were exposed to H/R stress in the presence or absence of recombinant human activin A protein and analyzed for markers of apoptotic cell death. As shown in Figure 2A, recombinant activin A protein promoted survival in NRVMs as assessed by an MTS assay. Statistically significant protection against apoptosis was observed when activin A was incubated with NRVMs at a dose

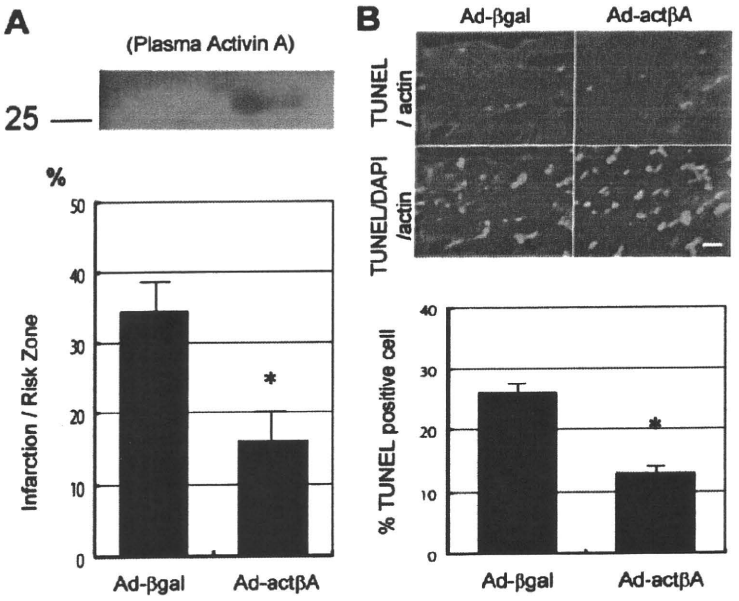

Figure 5. Adenovirus-mediated overexpression of activin A protects the heart from I/R injury. A, Representative Western blot analysis, performed under nonreducing conditions, of plasma samples collected 3 days after injection of Ad-βgal or Ad-actβA. Histogram shows quantification of infarct area induced by I/R 3 days after adenoviral injection. *$P<0.05$. B, Representative images of myocardium stained with TUNEL (green) and sarcomeric actin (red) (top panels) and merged with DAPI (blue) (bottom panels). Histogram shows quantification of TUNEL-positive cells in the myocardium after I/R. *$P<0.05$.

of 25 ng/mL. This level of activin A is similar to doses that exert antiapoptotic actions on other cell types.[20] To corroborate these findings, a nucleosome fragmentation assay of NRVM apoptosis was performed. Treatment with 25 ng/mL activin A reduced H/R-induced apoptosis by 62% (Figure 2B). Furthermore, caspase 3/7 activity was increased by the H/R stress, and treatment with activin A protein (25 ng/mL) reduced this activity to near baseline levels (Figure 2C).

Activin A signals through activin receptor-like kinases (ALKs).[1] Thus, NRVMs exposed to H/R stress were incubated with SB431542, a specific inhibitor of ALK4, ALK5, and ALK7, before treatment with recombinant activin A. Cell viability was assessed by MTS assay. As shown in Figure 2D, treatment with SB431542 abrogated the protective effect of activin A, whereas the inhibitor had no effect on basal cell viability. These data suggest that extracellular activin A protects cardiac myocytes from stress-induced apoptosis through the activities of ALKs.

To test whether Bcl-2 is involved in the antiapoptotic action of activin A in cardiac myocytes, Bcl-2 protein expression was determined by Western blot analysis. Activin A treatment significantly increased Bcl-2 protein levels in NRVMs (Figure 3A). Transduction of NRVMs with small interfering RNA (siRNA) targeting Bcl-2 reduced Bcl-2 protein expression. Knockdown of Bcl-2 with siRNA blocked the inhibitory effect of activin A on H/R-induced nucleosome fragmentation (Figure 3B). Thus, activin A cytoprotection is mediated by induction of Bcl-2.

Adenovirus-Mediated Expression of Activin A Promotes Myocyte Survival In Vitro and In Vivo

To corroborate and extend the findings obtained with the recombinant human activin A protein, an adenoviral vector that expresses the mouse *activin βA* gene (Ad-actβA) was generated. As shown in Figure 4A, transduction with Ad-actβA promoted the expression of Bcl-2 protein and increased the phosphorylation of Smad2 in NRVMs. The magnitude of these effects was similar to that observed with the recombinant activin A protein (Figure 3A). Transduction of NRVMs with Ad-actβA suppressed apoptosis induced by H/R as assessed by a nucleosome fragmentation assay (Figure 4B) and an MTS assay of cell viability (Figure 4C).

To examine the consequences of activin A on cardiac myocyte viability in vivo, mice were injected intravenously with ad-actβA or the control vector Ad-βgal. This method of intravenous delivery of adenoviral vectors leads to transduction of the liver but not heart, and secreted adenovirus-encoded proteins can be detected in the serum.[10,21] Mice receiving Ad-actβA exhibited detectable activin A protein expression in serum as assessed by Western blot analysis (Figure 5A). In response to myocardial I/R injury, mice treated with Ad-actβA displayed a 53.7% reduction in infarct size. This reduction corresponded to a decrease in the number of terminal deoxynucleotidyl transferase–mediated dUTP nick-end labeling (TUNEL)–positive, apoptotic cells in the area at risk of the Ad-actβA–treated group (Figure 5B). Collectively, these data show that activin A protects myocytes from apoptosis in vitro and in vivo and that it minimizes damage from I/R injury in the heart.

Fstl3 Inhibits Activin A–Mediated Protection of NRVMs

An adenoviral vector expressing the mouse *Fstl3* gene (Ad-Fstl3) was constructed because this factor is also induced by myocardial injury (Figure 1A to 1C), and it functions as an extracellular binding partner of activin A. Transduction of NRVMs with Ad-Fstl3 abrogated the ability of activin A protein to induce Smad2 phosphorylation (Figure 6A). In contrast, adenovirus-mediated overexpression of Fstl1 had no effect on activin A–induced Smad2 phosphorylation in NRVMs (Figure 6B).

Because Fstl3 is an inhibitor of activin A, we examined the effects of adeno-mediated induction of Fstl3 on activin A–mediated protection of NRVMs from stress-induced apoptosis. As

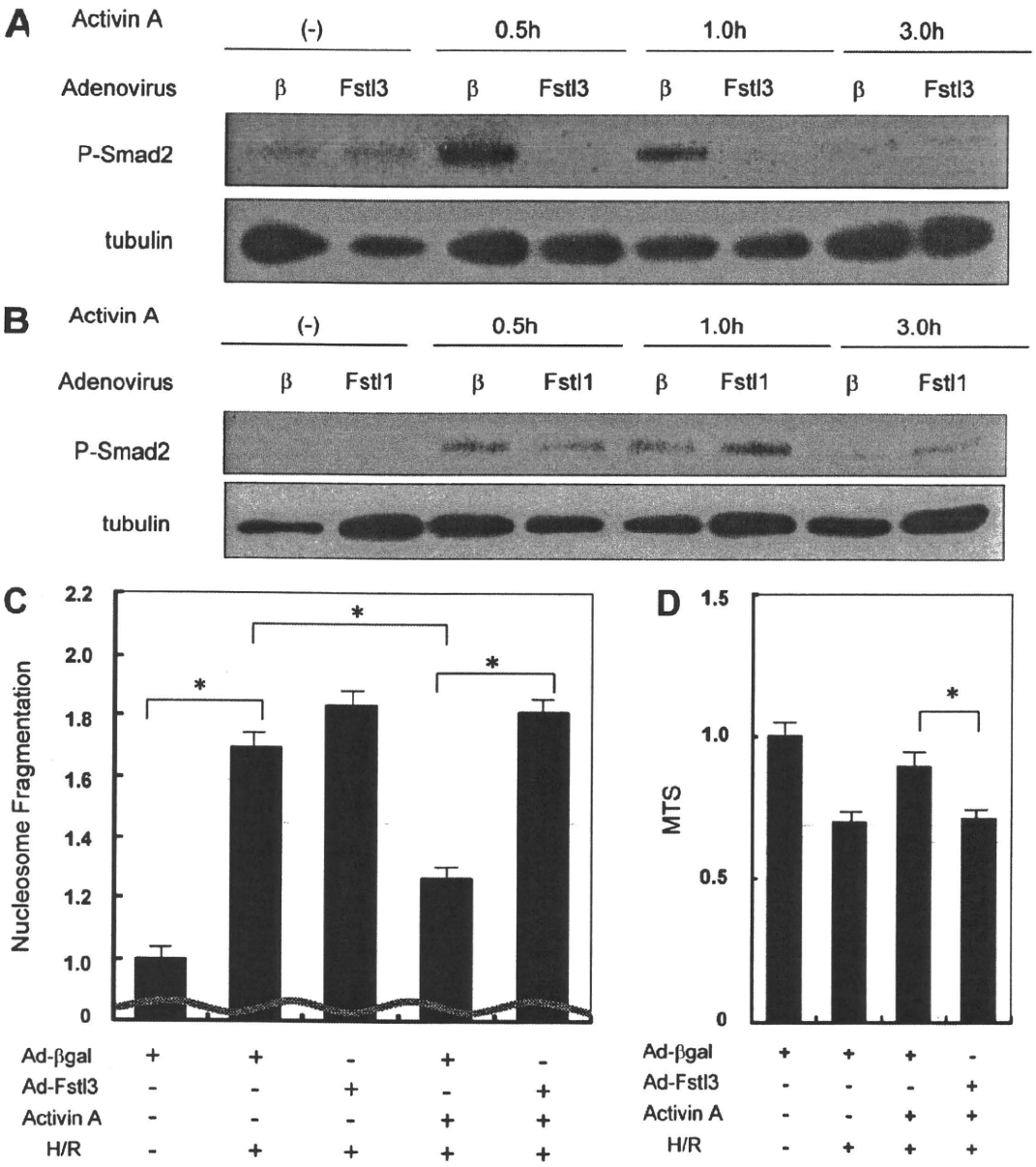

Figure 6. Fstl3 inhibits activin A action in NRVMs. A and B, NRVMs, transduced with Ad-Fstl3, Ad-Fstl1 or Ad-βgal (β) at 50 MOI, were stimulated with 25 ng/mL of recombinant activin A for indicated periods of time, and phosphorylation of Smad2 was determined by Western blot analysis. Immunoblots for α-tubulin were performed as a loading control. C and D, NRVMs were transduced with Ad-Fstl3 or Ad-βgal at an MOI of 50 (C) or 10 (D) and exposed to H/R treatment in the presence or absence of pretreatment with 25 ng/mL of activin A. Apoptosis was examined by nucleosome fragmentation assay (C), and cell viability was assessed by the MTS assay (D). *$P<0.05$.

shown by nucleosome fragmentation assay, transduction of Ad-Fstl3 abolished the prosurvival actions of activin A on NRVMs exposed to H/R stress (Figure 6C). The ability of Ad-Fstl3 to block activin A–mediated NRVM survival was corroborated by the MTS cell viability assay (Figure 6D).

Ablation of *Fstl3* in Cardiac Myocytes Protects the Heart From I/R Injury In Vivo

Cardiac myocyte–specific knockout mice for *Fstl3* were generated by crossing $Fstl3^{flox/flox}$ mice with mice expressing Cre recombinase from the α-MHC promoter. Cre-mediated recombination of the *Fstl3* allele in the hearts of α-MHC-Cre×$Fstl3^{flox/flox}$ (CKO) mice was confirmed by polymerase chain reaction (Figure I in the online-only Data Supplement). Quantitative real-time polymerase chain reaction analysis on the extracts from whole heart revealed a significant but incomplete reduction of *Fstl3* expression in CKO mice (Cre-f/f) compared with wild-type (W-f/f) mice (Figure 7A). Thus, cardiac myocytes were isolated from adult hearts of both strains of mice and evaluated for *Fstl3* expression (Figure 7B). Myocytes isolated from CKO mice were completely void of *Fstl3* transcript. Because whole-body *Fstl3*-deficient mice exhibit mild cardiac hypertrophy,[22] we evaluated the ratio of heart weight to body weight in the 2 strains

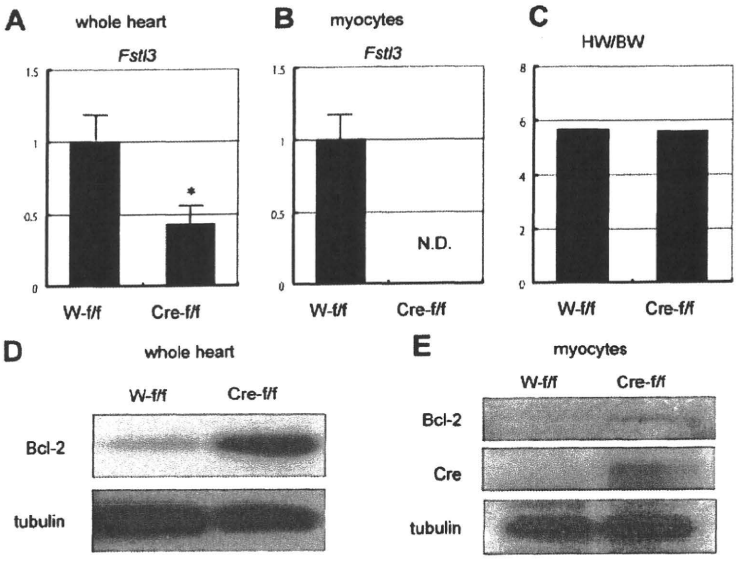

Figure 7. Fstl3 ablation in heart. A and B, Quantitative real-time polymerase chain reaction was performed to evaluate *Fslt3* mRNA expression in hearts of wild-type (W) or α-MHC-Cre (Cre) mice crossed with Fstl3$^{flox/flox}$ mice with the use of cDNA produced from whole heart extracts (A) or isolated cardiac myocytes (B). *$P<0.05$. C, Heart weight/body weight ratio (HW/BW) in 8-week-old male mice. D and E, Representative images of immunoblots of Bcl-2 expression in whole heart lysates (D) and isolated adult mouse cardiac myocytes (E). Immunoblots for α-tubulin are shown as a loading control.

of mice (Figure 7C). Cardiac myocyte–specific Fstl3 knockout mice did not show any difference in heart weight compared with wild-type mice. Western immunoblot analysis revealed the upregulation of Bcl-2 protein expression in CKO mice. The upregulation of Bcl-2 expression was also detected by Western immunoblot analysis of isolated cardiac myocytes from CKO hearts.

To examine the functional significance of *Fstl3* in myocytes of the heart, CKO and control mice hearts were subjected to I/R injury, and infarct size was analyzed by 2,3,5-triphenyltetrazolium chloride staining. As shown in Figure 8A, CKO hearts displayed smaller infarct zones, whereas the ratio of risk area to left ventricular area did not differ between the 2 groups (not shown). TUNEL analysis of the area at risk revealed fewer apoptotic cells in the Fstl3 CKO mice (Figure 8B).

Discussion

The heart secretes factors to maintain homeostasis and adapt to stress.[23–25] In the present study, we characterize the function of 2 new members of the cardiac secretome, Fstl3 and activin A. Fstl3 binds to activin A and other members of this family and inhibits their ability to activate signaling within target cells.[1] It has been reported that serum activin A levels and *Fstl3* transcript levels are elevated in heart failure,[9,14] but the regulatory functions of these factors in heart have not been examined previously. In this study, we show that both *Fstl3* and *Activin βA* mRNA are markedly upregulated in mouse heart in response to multiple types of injury. Functional analyses in vivo and in vitro showed that activin A is cardioprotective, whereas Fstl3 acts to nullify the protective action of activin A. These data indicate that the balance of expression between these 2 molecules can influence how the heart adapts to stress.

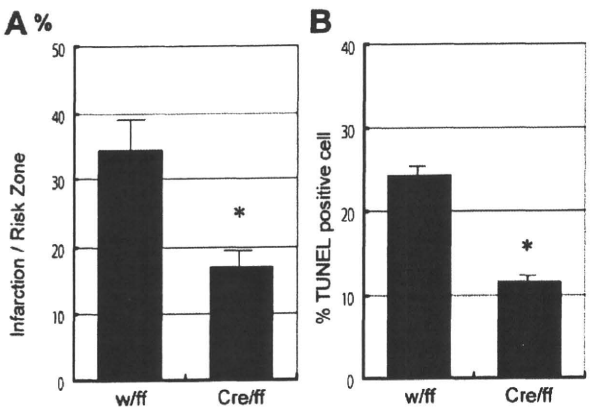

Figure 8. Ablation of Fstl3 protects the heart from I/R injury. A, Quantification of infarction size of *Fstl3*$^{flox/flox}$ crossed with wild-type (W/ff) or α-MHC-Cre (Cre/ff) after I/R injury. *$P<0.05$. B, Quantification of TUNEL-positive cells in the myocardium or control (W/ff) and CKO (Cre/ff) mice after I/R injury. *$P<0.05$.

Activin A is involved in numerous biological processes including embryonic development,[26] erythropoiesis,[27] wound healing,[28,29] cancer-related cachexia,[30] and inflammation.[31] Although it has been demonstrated that activin A is a prosurvival factor for neuronal cells,[15–17,20] other studies have demonstrated that activin A is a proapoptotic factor for hematopoietic cells[18] and adrenocortical carcinoma cells.[19] It has also been reported that inhibition of activin A by follistatin attenuates apoptosis induced by carbon tetrachloride injury in liver.[32] Thus, the mode of activin A action is highly dependent on tissue and cell type. In the present study, we present multiple lines of evidence showing that activin A is cardioprotective. In cultured cardiac myocytes subjected to stress, treatment with recombinant activin A protein upregulated Bcl-2 protein expression and reduced caspase activation and cellular apoptosis. Consistent with these results, adenovirus-mediated activin A overexpression promoted Bcl-2 expression and myocyte viability. Adenovirus-mediated expression of activin A also reduced infarct size and the frequency of TUNEL-positive cells in hearts that underwent I/R injury.

The functional significance of Bcl-2 induction by activin A was assessed by siRNA knockdown experiments in vitro. Treatment with siRNA directed at Bcl-2 effectively ablated activin A–stimulated expression of this protein by cultured

myocytes and blocked the cytoprotection actions of activin A. Previous studies have shown that Bcl-2 has roles in promoting cardiac myocyte viability in models of ischemic injury[33] and desmin deficiency–induced cardiomyopathy.[34] It has also been reported that activin A induces both Bcl-2 and Bcl-xL in neuroblastoma and pheochromocytoma cells.[20] However, we did not detect activin A–stimulated Bcl-xL expression in cardiac myocyte cultures (data not shown).

In this study, it is shown that Fstl3 inhibits the protective actions of activin A on cardiac myocytes. Pretreatment with an adenoviral vector expressing Fstl3 abrogates activin A–mediated suppression of NRVM death under conditions of H/R. Furthermore, cardiac myocyte–specific ablation of Fslt3 reduces infarct size and diminishes the frequency of apoptotic myocytes in the area at risk after I/R injury.

We previously showed that Fstl1 is upregulated by cardiac injuries in murine models,[10] and Lara-Pezzi et al reported that the *Fstl1* transcript is upregulated in human heart failure.[9] In contrast to Fstl3, Fstl1 protects cardiac myocytes from death both in vitro and in vivo.[10] Also in contrast to Fslt3, it is shown here that Fstl1 does not interfere with activin A–stimulated Smad2 phosphorylation (Figure 6). In contrast, Fstl1 protection of both cardiac myocytes and endothelial cells is dependent on the upregulation of Akt signaling.[10,35] Currently, there is no evidence to suggest that Fstl1 functions by binding to TGF-β superfamily members.

It was previously reported that whole-body *Fstl3* deficiency results in a low degree of cardiac hypertrophy accompanied by mildly elevated blood pressure in old female mice.[22] In the present study, we employed cardiac-specific Fstl3-deficient mice, and no change in ratio of heart weight to body weight was observed between CKO and wild-type mice. Because elevated blood pressure can lead to cardiac hypertrophy, the cardiac phenotype of the whole-body Fstl3 knockout mouse may be caused by the indirect actions of whole-body *Fstl3* deficiency on the heart.

Other TGF-β family cytokines reported to be produced by the heart under conditions of stress include myostatin/GDF-8 and GDF-15.[6–8,36] Like activin A, these factors regulate Smad signaling and cause cachexia when administered or overexpressed.[30,37,38] Both activin A and GDF-15 have been shown to be increased in patients with heart diseases.[14,39,40] Collectively, these studies indicate the existence of a broad signaling network involving TGF-β family factors and their extracellular inhibitory proteins that control cardiac adaptation to stress. The expression of these proteins by the damaged heart may also contribute to the systemic wasting response in chronic heart failure.

Conclusions

We show that activin A and its extracellular inhibitory protein Fstl3 are upregulated in murine heart under conditions of stress. Administration or overexpression of activin A protects myocytes from stress in vitro and in vivo. In contrast, Fstl3 overexpression inhibits the myocyte-protective activity of activin A in vitro, and cardiac-specific Fstl3-deficient mice display smaller infarcts and less myocyte apoptosis in response to I/R injury. Thus, we propose that activin A and Fstl3 function in an opposing manner to regulate myocyte survival and that the relative expression levels of these factors influence the adaptive response of the heart to injury.

Sources of Funding

This study was funded by National Institutes of Health grants HL77774, HL86785, AG15052, and HL81587 to K. Walsh. N. Ouchi was supported by American Heart Association grant 0635593T. D.R. Pimentel was supported by National Institutes of Health grant HL71563. Y. Oshima was supported by American Heart Association grant 0625867T. S. Lee was supported by National Institutes of Health grant U54-AR052646. K.D. Panse was supported by an EMBO fellowship (ASTF 53.00-2009).

Disclosures

None.

References

1. Shi Y, Massague J. Mechanisms of TGF-beta signaling from cell membrane to the nucleus. *Cell*. 2003;113:685–700.
2. Schultz Jel J, Witt SA, Glascock BJ, Nieman ML, Reiser PJ, Nix SL, Kimball TR, Doetschman T. TGF-beta1 mediates the hypertrophic cardiomyocyte growth induced by angiotensin II. *J Clin Invest*. 2002;109:787–796.
3. Okada H, Takemura G, Kosai K, Li Y, Takahashi T, Esaki M, Yuge K, Miyata S, Maruyama R, Mikami A, Minatoguchi S, Fujiwara T, Fujiwara H. Postinfarction gene therapy against transforming growth factor-beta signal modulates infarct tissue dynamics and attenuates left ventricular remodeling and heart failure. *Circulation*. 2005;111:2430–2437.
4. Izumi M, Fujio Y, Kunisada K, Negoro S, Tone E, Funamoto M, Osugi T, Oshima Y, Nakaoka Y, Kishimoto T, Yamauchi-Takihara K, Hirota H. Bone morphogenetic protein-2 inhibits serum deprivation-induced apoptosis of neonatal cardiac myocytes through activation of the Smad1 pathway. *J Biol Chem*. 2001;276:31133–31141.
5. Masaki M, Izumi M, Oshima Y, Nakaoka Y, Kuroda T, Kimura R, Sugiyama S, Terai K, Kitakaze M, Yamauchi-Takihara K, Kawase I, Hirota H. Smad1 protects cardiomyocytes from ischemia-reperfusion injury. *Circulation*. 2005;111:2752–2759.
6. Xu J, Kimball TR, Lorenz JN, Brown DA, Bauskin AR, Klevitsky R, Hewett TE, Breit SN, Molkentin JD. GDF15/MIC-1 functions as a protective and antihypertrophic factor released from the myocardium in association with SMAD protein activation. *Circ Res*. 2006;98:342–350.
7. Kempf T, Eden M, Strelau J, Naguib M, Willenbockel C, Tongers J, Heineke J, Kotlarz D, Xu J, Molkentin JD, Niessen HW, Drexler H, Wollert KC. The transforming growth factor-beta superfamily member growth-differentiation factor-15 protects the heart from ischemia/reperfusion injury. *Circ Res*. 2006;98:351–360.
8. Morissette MR, Cook SA, Foo S, McKoy G, Ashida N, Novikov M, Scherrer-Crosbie M, Li L, Matsui T, Brooks G, Rosenzweig A. Myostatin regulates cardiomyocyte growth through modulation of Akt signaling. *Circ Res*. 2006;99:15–24.
9. Lara-Pezzi E, Felkin LE, Birks EJ, Sarathchandra P, Panse KD, George R, Hall JL, Yacoub MH, Rosenthal N, Barton PJ. Expression of follistatin-related genes is altered in heart failure. *Endocrinology*. 2008;149:5822–5827.
10. Oshima Y, Ouchi N, Sato K, Izumiya Y, Pimentel DR, Walsh K. Follistatin-like 1 is an Akt-regulated cardioprotective factor that is secreted by the heart. *Circulation*. 2008;117:3099–3108.
11. Schiekofer S, Shiojima I, Sato K, Galasso G, Oshima Y, Walsh K. Microarray analysis of Akt1 activation in transgenic mouse hearts reveals transcript expression profiles associated with compensatory hypertrophy and failure. *Physiol Genomics*. 2006;27:156–170.
12. Schiekofer S, Belisle K, Galasso G, Schneider JG, Boehm BO, Burster T, Schmitz G, Walsh K. Angiogenic-regulatory network revealed by molecular profiling heart tissue following Akt1 induction in endothelial cells. *Angiogenesis*. 2008;11:289–299.
13. Shibata R, Sato K, Pimentel DR, Takemura Y, Kihara S, Ohashi K, Funahashi T, Ouchi N, Walsh K. Adiponectin protects against myocardial ischemia-reperfusion injury through AMPK- and COX-2-dependent mechanisms. *Nat Med*. 2005;11:1096–1103.
14. Yndestad A, Ueland T, Oie E, Florholmen G, Halvorsen B, Attramadal H, Simonsen S, Froland SS, Gullestad L, Christensen G, Damas JK, Aukrust

P. Elevated levels of activin A in heart failure: potential role in myocardial remodeling. *Circulation*. 2004;109:1379–1385.
15. Hughes PE, Alexi T, Williams CE, Clark RG, Gluckman PD. Administration of recombinant human activin-A has powerful neurotrophic effects on select striatal phenotypes in the quinolinic acid lesion model of Huntington's disease. *Neuroscience*. 1999;92:197–209.
16. Wu DD, Lai M, Hughes PE, Sirimanne E, Gluckman PD, Williams CE. Expression of the activin axis and neuronal rescue effects of recombinant activin A following hypoxic-ischemic brain injury in the infant rat. *Brain Res*. 1999;835:369–378.
17. Schubert D, Kimura H, LaCorbiere M, Vaughan J, Karr D, Fischer WH. Activin is a nerve cell survival molecule. *Nature*. 1990;344:868–870.
18. Valderrama-Carvajal H, Cocolakis E, Lacerte A, Lee EH, Krystal G, Ali S, Lebrun JJ. Activin/TGF-beta induce apoptosis through Smad-dependent expression of the lipid phosphatase SHIP. *Nat Cell Biol*. 2002;4:963–969.
19. Vanttinen T, Liu J, Kuulasmaa T, Kivinen P, Voutilainen R. Expression of activin/inhibin signaling components in the human adrenal gland and the effects of activins and inhibins on adrenocortical steroidogenesis and apoptosis. *J Endocrinol*. 2003;178:479–489.
20. Kupershmidt L, Amit T, Bar-Am O, Youdim MB, Blumenfeld Z. The neuroprotective effect of Activin A and B: implication for neurodegenerative diseases. *J Neurochem*. 2007;103:962–971.
21. Shibata R, Sato K, Kumada M, Izumiya Y, Sonoda M, Kihara S, Ouchi N, Walsh K. Adiponectin accumulates in myocardial tissue that has been damaged by ischemia-reperfusion injury via leakage from the vascular compartment. *Cardiovasc Res*. 2007;74:471–479.
22. Mukherjee A, Sidis Y, Mahan A, Raher MJ, Xia Y, Rosen ED, Bloch KD, Thomas MK, Schneyer AL. FSTL3 deletion reveals roles for TGF-beta family ligands in glucose and fat homeostasis in adults. *Proc Natl Acad Sci U S A*. 2007;104:1348–1353.
23. Shiojima I, Sato K, Izumiya Y, Schiekofer S, Ito M, Liao R, Colucci WS, Walsh K. Disruption of coordinated cardiac hypertrophy and angiogenesis contributes to the transition to heart failure. *J Clin Invest*. 2005;115:2108–2118.
24. Frost RJ, Engelhardt S. A secretion trap screen in yeast identifies protease inhibitor 16 as a novel antihypertrophic protein secreted from the heart. *Circulation*. 2007;116:1768–1775.
25. Izumiya Y, Shiojima I, Sato K, Sawyer DB, Colucci WS, Walsh K. Vascular endothelial growth factor blockade promotes the transition from compensatory cardiac hypertrophy to failure in response to pressure overload. *Hypertension*. 2006;47:887–893.
26. Matzuk MM, Kumar TR, Vassalli A, Bickenbach JR, Roop DR, Jaenisch R, Bradley A. Functional analysis of activins during mammalian development. *Nature*. 1995;374:354–356.
27. Murata M, Eto Y, Shibai H, Sakai M, Muramatsu M. Erythroid differentiation factor is encoded by the same mRNA as that of the inhibin beta A chain. *Proc Natl Acad Sci U S A*. 1988;85:2434–2438.
28. Munz B, Smola H, Engelhardt F, Bleuel K, Brauchle M, Lein I, Evans LW, Huylebroeck D, Balling R, Werner S. Overexpression of activin A in the skin of transgenic mice reveals new activities of activin in epidermal morphogenesis, dermal fibrosis and wound repair. *EMBO J*. 1999;18:5205–5215.
29. Wankell M, Munz B, Hubner G, Hans W, Wolf E, Goppelt A, Werner S. Impaired wound healing in transgenic mice overexpressing the activin antagonist follistatin in the epidermis. *EMBO J*. 2001;20:5361–5372.
30. Matzuk MM, Finegold MJ, Mather JP, Krummen L, Lu H, Bradley A. Development of cancer cachexia-like syndrome and adrenal tumors in inhibin-deficient mice. *Proc Natl Acad Sci U S A*. 1994;91:8817–8821.
31. Jones KL, Mansell A, Patella S, Scott BJ, Hedger MP, de Kretser DM, Phillips DJ. Activin A is a critical component of the inflammatory response, and its binding protein, follistatin, reduces mortality in endotoxemia. *Proc Natl Acad Sci U S A*. 2007;104:16239–16244.
32. Patella S, Phillips DJ, Tchongue J, de Kretser DM, Sievert W. Follistatin attenuates early liver fibrosis: effects on hepatic stellate cell activation and hepatocyte apoptosis. *Am J Physiol*. 2006;290:G137–G144.
33. Imahashi K, Schneider MD, Steenbergen C, Murphy E. Transgenic expression of Bcl-2 modulates energy metabolism, prevents cytosolic acidification during ischemia, and reduces ischemia/reperfusion injury. *Circ Res*. 2004;95:734–741.
34. Weisleder N, Taffet GE, Capetanaki Y. Bcl-2 overexpression corrects mitochondrial defects and ameliorates inherited desmin null cardiomyopathy. *Proc Natl Acad Sci U S A*. 2004;101:769–774.
35. Ouchi N, Oshima Y, Ohashi K, Higuchi A, Ikegami C, Izumiya Y, Walsh K. Follistatin-like 1, a secreted muscle protein, promotes endothelial cell function and revascularization in ischemic tissue through a nitric-oxide synthase-dependent mechanism. *J Biol Chem*. 2008;283:32802–32811.
36. Sharma M, Kambadur R, Matthews KG, Somers WG, Devlin GP, Conaglen JV, Fowke PJ, Bass JJ. Myostatin, a transforming growth factor-beta superfamily member, is expressed in heart muscle and is upregulated in cardiomyocytes after infarct. *J Cell Physiol*. 1999;180:1–9.
37. Zimmers TA, Davies MV, Koniaris LG, Haynes P, Esquela AF, Tomkinson KN, McPherron AC, Wolfman NM, Lee SJ. Induction of cachexia in mice by systemically administered myostatin. *Science*. 2002;296:1486–1488.
38. Johnen H, Lin S, Kuffner T, Brown DA, Tsai VW, Bauskin AR, Wu L, Pankhurst G, Jiang L, Junankar S, Hunter M, Fairlie WD, Lee NJ, Enriquez RF, Baldock PA, Corey E, Apple FS, Murakami MM, Lin EJ, Wang C, During MJ, Sainsbury A, Herzog H, Breit SN. Tumor-induced anorexia and weight loss are mediated by the TGF-beta superfamily cytokine MIC-1. *Nat Med*. 2007;13:1333–1340.
39. Kempf T, von Haehling S, Peter T, Allhoff T, Cicoira M, Doehner W, Ponikowski P, Filippatos GS, Rozentryt P, Drexler H, Anker SD, Wollert KC. Prognostic utility of growth differentiation factor-15 in patients with chronic heart failure. *J Am Coll Cardiol*. 2007;50:1054–1060.
40. Wollert KC, Kempf T, Peter T, Olofsson S, James S, Johnston N, Lindahl B, Horn-Wichmann R, Brabant G, Simoons ML, Armstrong PW, Califf RM, Drexler H, Wallentin L. Prognostic value of growth-differentiation factor-15 in patients with non-ST-elevation acute coronary syndrome. *Circulation*. 2007;115:962–971.

CLINICAL PERSPECTIVE

The injured heart secretes proteins that influence its function. In this study, we characterize 2 new members of the cardiac "secretome," activin A and follistatin-like 3 (Fstl3), using genetic gain- and loss-of-function manipulations in mouse models. Activin A and Fstl3 expression was increased in heart after various injuries and in cultured myocytes after hypoxia/reoxygenation. Activin A protected myocytes from cell death, and this protective activity was antagonized by Fstl3, which functions as an extracellular inhibitory protein for activin A. Myocardial ischemia/reperfusion injury was reduced in mice administered activin A. Genetic ablation of Fstl3 in cardiac myocytes also diminished injury in response to ischemia/reperfusion. We speculate that activin A and Fstl3 serve as sensors of cardiac stress and that their relative levels of expression influence the adaptive response of the heart to injury.

Supplemental Material

Supplemental Methods

Reagents. SYBR GREEN was purchased from Applied Biosystems. The adenoviral backbone plasmid pAdEasy-1 was obtained from Qbiogene. Antibodies against phospho-Smad2 (Ser465/467), phospho-Smad1/5/8 (Ser463/465), phospho-Akt1 (Ser473), phospho-AMPK (Thr172) and phospho-ERK (Thr202/Tyr204) were purchased from Cell Signaling Technology. Anti-mouse Fstl-3 and Activin βA antibodies were obtained from R&D Systems. Antibody against alpha-tubulin was purchased from Calbiochem, Bcl2 was from BD Transduction Laboratories and sarcomeric actin was from Sigma. Dulbecco's modified Eagle's medium (DMEM) and MEM were purchased from Invitrogen. Liberase blendzyme 4 was obtained from Roche. SB431542 was from Calbiochem. Recombinant human Activin A (rActA) (expressed in CHO cells) and taurine were purchased from Sigma.

RNA isolation, reverse transcriptional PCR, and Quantitative Real-Time PCR. Total RNA preparation from mouse heart was carried out by using RNA isolation kit for fibrous tissue (Qiagen) and preparation from cultured cells was performed by RNA isolation kit (Qiagen) according to manufacturer's protocols. We synthesized cDNA from 450 ng of total RNA by using ThermoScript RT-PCR Systems (Invitrogen) according to the manufacturer's instructions. Quantitative Real-Time PCR (QRT-PCR) was carried out on an iCycler (Bio-Rad). SYBR GREEN 1 was used as a double-stranded DNA-specific dye according to the manufacture's instruction (Applied Biosystems)[1]. We designed primers to be suitable for a single QRT-PCR thermal profile (95 °C for 10 min, and 50

cycles of 95 °C for 30 s and 60 °C for 1 min). The sequences are as follows: *glyceraldehyde- 3-phosphate dehydrogenase (GAPDH)* forward (F) : 5'-TCACCACCATGGAGAAGGC-3' reverse (R) : 5' - GCTAAGCAGTTGGTGGTGCA -3' *Actβ*A (forward) : 5'– TGGTGCCAGTCTAGTGCTTC -3' R: 5'–CCGTCACTCCCATCTTTCTT -3' *Inhibin α* F: 5'–TCCTTTTGCTGTTGACCCTA-3' R: 5'– CCCCAAGGCATCTAGGAATA -3' *Follistatin F* : 5'-CGAGGAGGATGTGAACGACAA-3' R : 5'-GGTCCGCAGTCCACGTTCT-3' Fstl3 F : 5'-CAACCCCGGCCAAGAACT-3' R : 5'-CTTCCTCCTCTGCTGGTACTTTG-3' The expression levels of examined transcripts were compared to that of GAPDH or 18S and normalized to the mean value of controls. Expression levels were compared to that of *GAPDH* and normalized to the mean value of controls.

Western immunoblot analysis. Heart tissue was homogenized in lysis buffer (Cell Signaling) containing 1 mM PMSF and protease inhibitors (Pierce). Cultured cells were directly lysed in the lysis buffer to obtain protein samples. Protein concentration was measured using BCA protein assay kit (Pierce). The cell and tissue lysates, culture media or serum were added to equal volumes of 2x sample buffer (BioRad), and separated by SDS-PAGE. For the detection of Activin A and Fstl3, protein from NRVM media was concentrated up to fifty fold by Microcon (Millipore). Mature Activin A protein was subjected to electrophoresis under non-reducing conditions. Proteins were transferred onto PVDF membrane (Amersham). western blot analysis was performed by probing with the primary antibody followed by incubation with the HRP-conjugated

secondary antibody. The ECL plus system (Amersham) was used to produce chemiluminescent signal.

Detection of nucleosome fragmentation by ELISA. Apoptosis was assessed by enzyme-linked immunosorbent assay (ELISA) based detection of nucleosome fragmentation by Cell Death Detection kit (Roche) as described previously[2]. NRVMs were seeded in 96-well plates, transfected with adenoviral vectors and exposed to H/R. For each assay, at least 8 wells for each experimental group were analyzed. The extent of nucleosome fragmentation of each group was compared to that of control group (e.g. no treatment or Ad-βgal transfected cells maintained at a normoxic condition) and normalized to the mean value of controls.

MTS assay. An MTS [3-(4,5-dimethylthiazol-2-yl)-5-(3-carboxymethoxyphenyl) -2-(4-sulfophenyl)-2H-tetrazolium] assay was carried out in NRVMs to evaluate cell viability using CellTiter 96 Aqueous One Solution Cell Proliferation Assay (Promega). Cells were incubated for two to three hours after addition of the reagent and absorbance was recorded. The relative cell viabilities were calculated as the ratio to that of control group. For each assay, at least 8 wells were measured for each experimental group, and assays were repeated three times.

Measurement of Caspase-3 and -7 activities. Caspase-3 and -7 activities in NRVMs were measured by Apo-ONE Homogeneous Caspase-3/7 Assay (Promega) according to the manufactures protocol. In brief, the buffer and substrate mixture was added into culture dishes and incubated for two hours. A fluorescent signal is detected upon

substrate cleavage by caspase-3 and -7. The excitation wavelength was 485 nm and the emission wavelength was 530 nm. The relative fluorescent intensities were calculated as the ratio to that of control group. For each assay, at least 8 wells were measured for each experimental group, and assays were repeated three times.

Mouse models. Eight to 10 week old male mice were used for ischemia-reperfusion surgery as described previously[3]. Following anesthetization (pentobarbital 50 mg/kg i.p.) and intubation, the chest was exteriorized and 8-0 monofilament suture was ligated around the proximal left coronary artery (LCA) using a snare occluder. Ischemia followed by reperfusion was accomplished by tightening the snare occluder for 30 min. Myocardial reperfusion was confirmed by changes in ECG as well as by changes in appearance of the heart from pale to bright red. The suture was left in place and chest was closed. During the surgical procedure, the body temperature was monitored and maintained at 37+/-1 °C. Twenty four hours after reperfusion, the chest was re-opened and the suture was re-tied. Evans Blue was injected at the aortic root to determine the area at risk (AAR). The heart was then excised and incubated with 2,3,5-triphenyltetrazolium chloride (TTC) for 5 min at 37 °C to determine the infarction area (IA). Left ventricular area (LVA), AAR and IA were determined by computerized planimetry using Image J (Bethesda, Maryland, USA). Tissue were harvested at 24 hours post-reperfusion for analysis of transcript levels. Mouse transverse aortic constriction was carried out as described previously[4]. In brief, following anesthetization, the chest was opened and intercostal muscles were dissected to reach to the aortic arch. The aortic arch was tied around a 26-gauge needle by a 7-0 silk suture. Tissue

was harvested at 1 week time point for analysis. In the mouse myocardial infarction model, the LCA was kept occluded and the chest was closed without reperfusion.

TUNEL staining. TUNEL staining on frozen heart sections was performed as described previously[5] with some modifications. Cryo-sections (6 μm thickness) were fixed with 4% paraformaldehyde in PBS, permeabilized with 0.1% Triton X-100 and blocked with 6% skim milk. Anti-sarcomeric actin antibody was used for determination of myocytes followed by TUNEL and nuclear staining as described above. TUNEL positive myocytes were counted in three randomly selected fields of the slide. Each experiment was repeated three times and each tissue section was processed in duplicate.

Isolation of adult mouse ventricular cardiac myocytes. Isolation of adult mouse ventricular cardiac myocytes was performed according to procedures described online from the Alliance for Cell Signaling (AfSC protocols, http://www.signaling-gateway.org/data/Data.html) and O'Connell et al. 2007[6]. Briefly, adult WT × Fstl3 $^{flox/flox}$ and αMHC-Cre × Fslt3 $^{flox/flox}$ mice were injected with 50 IU of heparin and anesthetized with isoflurane. The heart was immediately extracted and placed into perfusion buffer and cannulated. After perfusion with perfusion buffer, the buffer was switched to the digestion buffer containing 0.25 mg/ml Liberase blendzyme 4, 0.14 mg/ml Trypsin and 12.5 μM $CaCl_2$. After enzymatic digestion, the heart was disaggregated by forceps in the presence of a stop solution containing 10% Bovine Calf Serum to inactivate the protease. The tissue was further dissociated by gentle pipettings, and cells were collected by centrifugation. Cells were plated on laminin pre-coated 6-well culture plates and allowed to attach for 1 hour. Unattached cells were washed away. Attached rod-

shaped cardiac myocytes were incubated for another 24 hours in culture media (MEM with 0.1 mg/ml of bovine serum albumin, 100 U/ml of penicillin and 2 mM of L-Glutamine) at 37 °C in 2% CO_2 prior to use.

Supplemental Figure

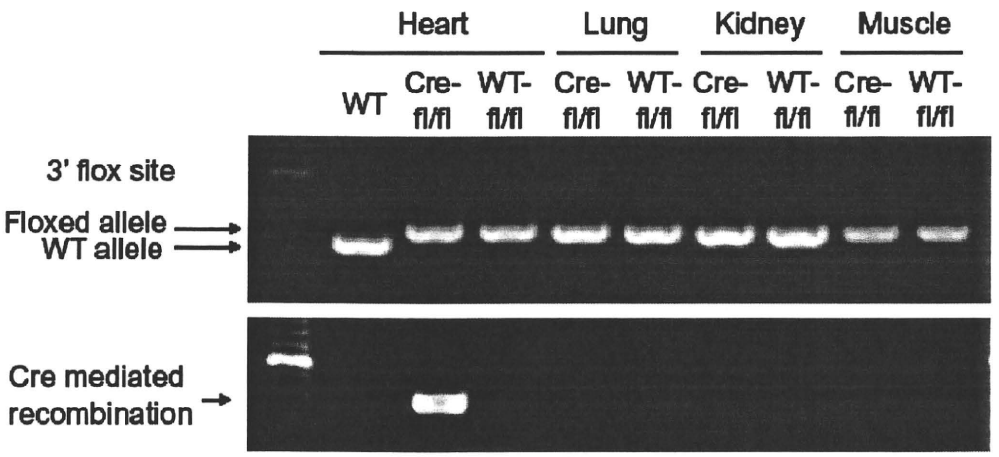

Supplemental Figure Legend

Expression of Cre recombinase and floxed allele in the heart. DNA was isolated from heart, lung, kidney and skeletal muscle in wild-type (WT), Cre-flox/flox (Cre-fl/fl) or WT-fl/fl mice. Cre recombinase and floxed allele were determined by PCR.

Supplemental References

1. Schiekofer S, Shiojima I, Sato K, Galasso G, Oshima Y, Walsh K. Microarray analysis of Akt1 activation in transgenic mouse hearts reveals transcript expression profiles associated with compensatory hypertrophy and failure. *Physiol Genomics* 2006; **27:** 156-70.

2. Oshima Y, Ouchi N, Sato K, Izumiya Y, Pimentel DR, Walsh K. Follistatin-like 1 is an Akt-regulated cardioprotective factor that is secreted by the heart. *Circulation* 2008; **117:** 3099-108.

3. Shibata R, Sato K, Pimentel DR, Takemura Y, Kihara S, Ohashi K et al. Adiponectin protects against myocardial ischemia-reperfusion injury through AMPK- and COX-2-dependent mechanisms. *Nat Med* 2005; **11:** 1096-103.

4. Shibata R, Ouchi N, Ito M, Kihara S, Shiojima I, Pimentel DR et al. Adiponectin-mediated modulation of hypertrophic signals in the heart. *Nat Med* 2004; **10:** 1384-9.

5. Fujio Y, Nguyen T, Wencker D, Kitsis RN, Walsh K. Akt promotes survival of cardiomyocytes in vitro and protects against ischemia-reperfusion injury in mouse heart. *Circulation* 2000; **101:** 660-7.

6. O'Connell TD, Rodrigo MC, Simpson PC. Isolation and culture of adult mouse cardiac myocytes. *Methods Mol Biol* 2007; **357:** 271-96.

Research

Activin plays a key role in the maintenance of long-term memory and late-LTP

Hiroshi Ageta,[1,2,3] Shiro Ikegami,[1] Masami Miura,[4] Masao Masuda,[4] Rika Migishima,[1] Toshiaki Hino,[1] Noriko Takashima,[1,2] Akiko Murayama,[1,2] Hiromu Sugino,[5] Mitsutoshi Setou,[1,6] Satoshi Kida,[2,7] Minesuke Yokoyama,[1,8] Yoshihisa Hasegawa,[9] Kunihiro Tsuchida,[3] Toshihiko Aosaki,[4] and Kaoru Inokuchi[1,2,8,10,11]

[1]*Mitsubishi Kagaku Institute of Life Sciences, MITILS, Machida, Tokyo 194-8511, Japan;* [2]*Japan Science and Technology Agency, CREST, Kawaguchi, Saitama 332-0012, Japan;* [3]*Institute for Comprehensive Medical Science, Fujita Health University, Aichi 470-1192, Japan;* [4]*Neuropathophysiology Research Group, Tokyo Metropolitan Institute of Gerontology, Tokyo 173-0015, Japan;* [5]*National Institute of Advanced Industrial Science and Technology, Tsukuba 305-8562, Japan;* [6]*Molecular Imaging Advanced Research Center, Department of Molecular Anatomy, Hamamatsu University School of Medicine, Hamamatsu, Shizuoka 431-3192, Japan;* [7]*Department of Agricultural Chemistry and Bioscience, Faculty of Applied Science, Tokyo University of Agriculture, Tokyo 156-8502, Japan;* [8]*Brain Research Institute, Niigata University, Niigata 951-8585, Japan;* [9]*Laboratory Animal Science, Kitasato University School of Veterinary Medicine and Animal Sciences, Towada, Aomori 034-8628, Japan;* [10]*Department of Biochemistry, Faculty of Medicine, Graduate School of Medicine and Pharmaceutical Sciences, University of Toyama, Toyama 930-0194, Japan*

A recent study has revealed that fear memory may be vulnerable following retrieval, and is then reconsolidated in a protein synthesis-dependent manner. However, little is known about the molecular mechanisms of these processes. Activin βA, a member of the TGF-β superfamily, is increased in activated neuronal circuits and regulates dendritic spine morphology. To clarify the role of activin in the synaptic plasticity of the adult brain, we examined the effect of inhibiting or enhancing activin function on hippocampal long-term potentiation (LTP). We found that follistatin, a specific inhibitor of activin, blocked the maintenance of late LTP (L-LTP) in the hippocampus. In contrast, administration of activin facilitated the maintenance of early LTP (E-LTP). We generated forebrain-specific activin- or follistatin-transgenic mice in which transgene expression is under the control of the Tet-OFF system. Maintenance of hippocampal L-LTP was blocked in the follistatin-transgenic mice. In the contextual fear-conditioning test, we found that follistatin blocked the formation of long-term memory (LTM) without affecting short-term memory (STM). Furthermore, consolidated memory was selectively weakened by the expression of follistatin during retrieval, but not during the maintenance phase. On the other hand, the maintenance of memory was also influenced by activin overexpression during the retrieval phase. Thus, the level of activin in the brain during the retrieval phase plays a key role in the maintenance of long-term memory.

[Supplemental material is available online at http://www.learnmem.org.]

Formation of long-term memory (LTM) consists of several distinct processes: acquisition, consolidation, and reconsolidation, through which memory becomes permanent (Nader et al. 2000; Rodrigues et al. 2004; Tronson and Taylor 2007; Kitamura et al. 2009). The prominent feature of LTM is a requirement for RNA and protein synthesis for consolidation and reconsolidation (Squire and Barondes 1973; Bourtchuladze et al. 1994; Silva et al. 1998; Tronson and Taylor 2007; Lee et al. 2008). The reconsolidation process may serve to strengthen or renew the original fear memory (Nader 2003; Tronson and Taylor 2007). Synaptic plasticity is thought to underlie memory formation. Recent studies have shown that the learning process induces long-term potentiation (LTP) (Rogan et al. 1997; Rioult-Pedotti et al. 2000), a form of synaptic plasticity, and, conversely, that LTP is necessary for memory formation (Rodrigues et al. 2004). Similar to LTM, LTP requires protein and RNA synthesis for its prolonged maintenance, late LTP (L-LTP) (Frey et al. 1988; Abraham et al. 1993; Nguyen et al. 1994; Fukazawa et al. 2003).

In order to understand the molecular mechanism of LTM, we previously isolated a number of neuronal activity-dependent genes, including *activin βA*, *ubiquitin C-terminal hydrolase*, *vesl-1S/homer-1a*, and *SCRAPPER* (Inokuchi et al. 1996; Hegde et al. 1997; Kato et al. 1997; Yao et al. 2007; Okada et al. 2009). *Activin βA*, a member of the TGF-β superfamily (Massague 1998), is one of the genes whose expression is up-regulated following L-LTP induction (Andreasson and Worley 1995; Inokuchi et al. 1996). Activin is a multifunctional ligand that regulates the proliferation and differentiation of numerous cell types (Mather et al. 1997; Ying et al. 1997). Activin binds to the serine/threonine kinase receptor activin type II (ActRII) that is located on the cell membrane (Pangas and Woodruff 2000). Once ligand is bound, the type II receptor recruits and phosphorylates an activin type I receptor (ActRI). Following stimulation by activin, the transcription factors Smad2 and Smad3 are phosphorylated by ActRI

[11]Corresponding author.
Email inokuchi@med.u-toyama.ac.jp; fax 81-76-434-5014
Article is online at http://www.learnmem.org/cgi/doi/10.1101/lm.16659010.

(Pangas and Woodruff 2000). Activin receptor ActRII is highly expressed in the forebrain region (Cameron et al. 1994; Funaba et al. 1997), and its scaffold protein ARIP/S-SCAM is also localized to the synaptic region (Hirao et al. 1998; Shoji et al. 2000).

Recent studies reveal that activin regulates the morphology of dendritic spines (Shoji-Kasai et al. 2007) and neurogenesis (Ageta et al. 2008; Abdipranoto-Cowley et al. 2009; Sekiguchi et al. 2009), has a neuroprotective function (Tretter et al. 2000), and plays a role in anxiety-related behavior (Dow et al. 2005; Ageta et al. 2008; Zheng et al. 2008). We previously found that activin increases the number of synaptic contacts and the length of dendritic spine necks by modulating spinal actin dynamics (Shoji-Kasai et al. 2007). We hypothesized that activin modulates spine actin dynamics and that this in turn affects LTP persistence. Furthermore, activin induces phosphorylation of the *N*-methyl-D-aspartate receptor (NMDAR), a key component in the formation of LTP (Nicoll and Malenka 1999), and increases Ca^{2+} influx through NMDAR (Kurisaki et al. 2008). This activin-induced NMDAR activation persists for >24 h. These results suggest that activin has an important role in the formation of L-LTP and LTM.

Results

Activin is indispensable for in vivo L-LTP

We examined the hippocampal dentate gyrus LTP of urethane-anesthetized rats. A strong high-frequency stimulation (HFS, five 400-pulse trains at 400 Hz) produced a long-lasting L-LTP in vivo that persisted for 24 h (Fig. 1A). However, when the activin inhibitor follistatin (0.5 μg) (Nakamura et al. 1990; Sugino et al. 1997) or an anti-activin A antibody (0.6 μg) was pre-injected into the lateral ventricle, the strong HFS induced an LTP that

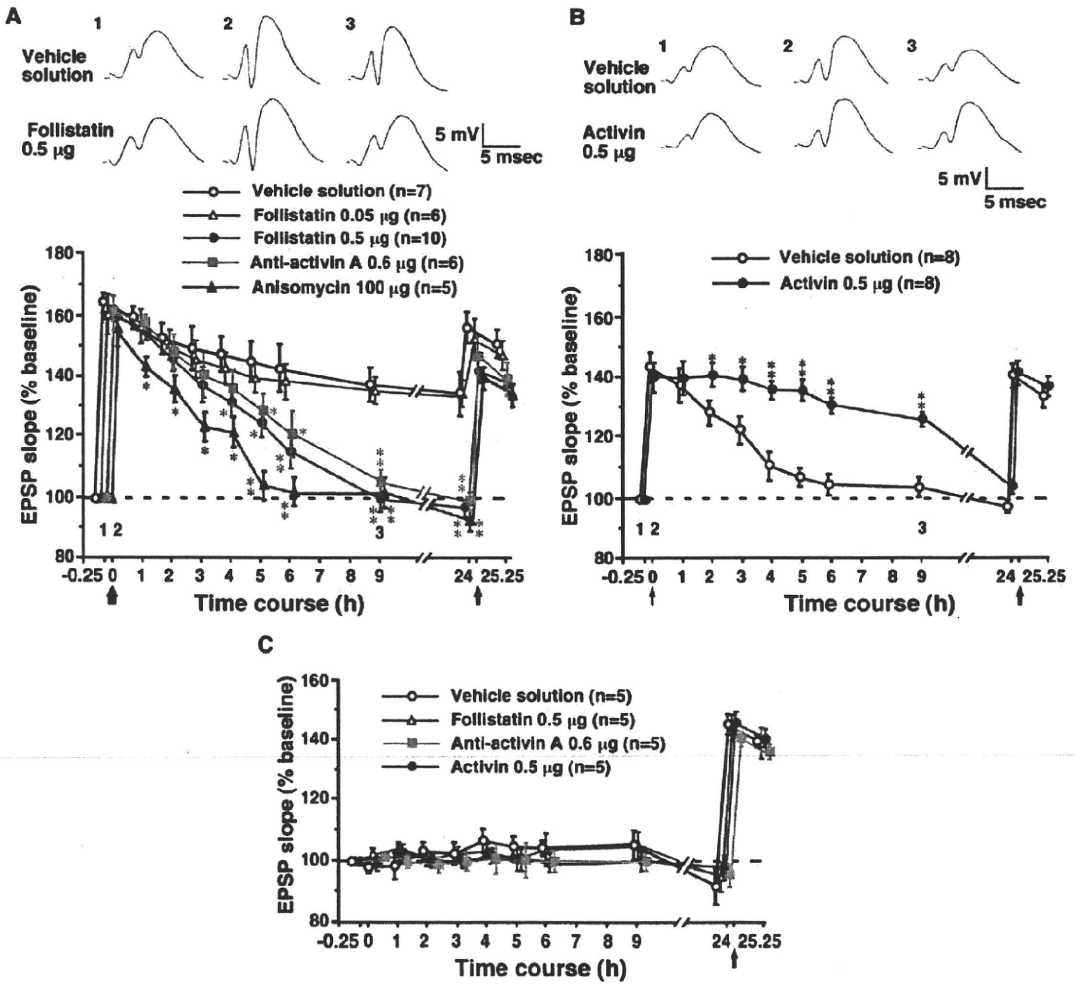

Figure 1. Activin is required for the maintenance of dentate gyrus L-LTP in vivo. (*A*) Effect of follistatin, anti-activin A, and anisomycin on LTP persistence. A strong HFS was delivered at time 0 (thick arrow). (*B*) Effect of activin on LTP persistence. A weak HFS was delivered at time 0 (thin arrow). (C) Basal synaptic transmission was not affected by follistatin, anti-activin A, or activin. The average of the fEPSP slope during the 15 min prior to time 0 served as the baseline (100%) for all trials. (*) $P < 0.05$, (**) $P < 0.005$ between the vehicle and experimental groups as determined by one-way ANOVA followed by Fisher's LSD test. At the end of each experiment, a second HFS (100 pulses at 100 Hz) was delivered (red arrows at 24 h). (*Top* panels in *A,B*) Typical fEPSP traces evoked at the times (1, 2, or 3) indicated in each graph. Error bars indicate SEM.

decayed rapidly and returned to basal levels by 9 h (Fig. 1A). The decay time course is similar to that of animals injected with the protein synthesis inhibitor anisomycin (Fig. 1A). In contrast, follistatin or anti-activin A had no significant effect on the initial amplitude and early maintenance of LTP (E-LTP). The effect of follistatin was dose-dependent because the injection of a lower dose (0.05 μg) did not alter the maintenance of L-LTP (Fig. 1A). To exclude the possibility that the LTP decay caused by follistatin or the anti-activin A antibody was due to irreversible damage to hippocampal neurons, a second HFS (100 pulses at 100 Hz) was applied to the same pathway at the end of each experiment (24 h). We observed an enhancement of the field excitatory postsynaptic potential (fEPSP) slope in all animals (Fig. 1A), which eliminates the possibility that neuronal damage occurred.

In a complementary experiment where activin was preinjected into the lateral ventricle, we used a weak HFS (a 50-pulse train at 100 Hz). The weak HFS alone elicited E-LTP that returned to the basal level by 6 h (Fig. 1B). However, pre-administration of activin facilitated the maintenance of LTP, since the weak HFS under these conditions produced an LTP that lasted >9 h. Injection of follistatin, anti-activin A, or activin into the lateral ventricle had no significant effect on basal synaptic transmission (Fig. 1C).

When injected 1 h after the delivery of the weak HFS, activin still enhanced E-LTP (Supplemental Fig. S1A). However, activin failed to facilitate LTP maintenance when administered 3 h after the weak HFS. Consistent with this result is the observation that the inhibitory effect of follistatin on L-LTP establishment was observed when it was injected 1 h, but not 3 h, after the delivery of the strong HFS (Supplemental Fig. S1B).

Generation of activin and follistatin transgenic mice using a forebrain-specific Tet-OFF system

To examine the role activin plays in fear memory formation, activin activity was genetically suppressed or increased in the forebrain of transgenic mice carrying a Tet-OFF system. In this system, the tetracycline-controlled transactivator (tTA) is under the control of the CaMKIIα promoter to achieve forebrain-specific expression (Fig. 2A; Mayford et al. 1996). We generated two distinct lines of responder mice, ABI and FBI, in which activin and follistatin, respectively, were controlled by the tetracycline response element (TRE) promoter. Double (FBItTA and ABItTA)-transgenic mice were obtained by heterozygous crossings. A diet containing DOX (6 mg/g food) was fed to pregnant mice for 7 consecutive days immediately prior to the expected date of confinement to reduce leak expression of follistatin or activin during the late embryonic stage. Double-transgenic ABItTA and FBItTA mice were fertile, bred normally, and maintained a normal body weight under the no-DOX treatment.

The tTA binds specifically to the TRE promoter and activates transcription in the absence of DOX (Mayford et al. 1996). In these mice, TRE bidirectionally regulated LacZ (Fig. 2A). Thus, LacZ activity was detected in some brain regions including the hippocampus, striatum, and amygdala in ABItTA, but not ABI, mice in the absence of DOX treatment. LacZ activity was also detected in some brain regions including the hippocampus and cortex in FBItTA, but not FBI, mice in the absence of DOX treatment (Fig. 2B; Supplemental Fig. S2). An ELISA analysis revealed that the activin level in the hippocampus of ABI mice (0.06 ng/mg protein, Fig. 2C) was equivalent to that of wild-type mice (Ageta et al. 2008), showing no leaky transgene expression in ABI mice. Moreover, the follistatin level in the hippocampus of FBItTA mice (0.25–0.5 ng/mg protein) was sufficient to antagonize the endogenous hippocampal activin (0.06 ng/mg protein) in the absence of DOX treatment (Sugino et al. 1997). DOX administration decreased the ectopic activin and follistatin to basal levels within 3 d in the hippocampus of ABItTA and FBItTA mice (Fig. 2C). Suppression by DOX was reversible and almost completely recovered within 3 d for FBItTA and 14 d for ABItTA (Fig. 2C). There was no significant difference in the activin level in the hippocampus of ABI and ABItTA mice on days 1 and 7 (Fig. 2C). No transgene expression was observed in the cerebellum and medulla of ABItTA and FBItTA mice in the absence of DOX treatment.

The maintenance of L-LTP is reduced in FBItTA mice

Hippocampal slices were prepared from 6- to 10-wk-old FBI and FBItTA mice, and fEPSPs were recorded in the hippocampal CA1 region after the application of single test stimulus every 20 sec (0.05 Hz) to the Schaffer collaterals. We first examined whether the basic property of excitatory synaptic transmission was normal in FBItTA mice. We measured the initial slope of fEPSP in order to quantify the strength of the synaptic response. The input–output relationship in FBItTA mice was similar to that of FBI mice (Fig. 3A). In the CA1 region, paired stimulation with short intervals usually causes paired-pulse facilitation (PPF). The extent of PPF with interpulse intervals of 25–500 msec of FBItTA mice was identical to that of FBI mice (Fig. 3B). These results suggest that there are no physiological differences in the basic properties of excitatory synaptic transmission between FBItTA and FBI mice.

We then examined whether E-LTP in the CA1 region was altered in FBItTA mice. After a baseline recording of at least 15 min, LTP was induced by tetanic stimulation. A single train of tetanic stimulation, 100 Hz for 1 sec, elicited identical E-LTP in both strains of mice (136.2 ± 14.0% and 144.8 ± 16.0%, 90–120 min after tetanic stimulation in FBItTA and FBI mice, respectively). Three trains of tetanic stimulation at 20-sec intervals caused much larger E-LTP than that after a single train of tetanus, but E-LTP in FBItTA mice was similar to that in FBI mice (161.8 ± 9.3% and 175.8 ± 8.0%, 90–120 min after tetanic stimulation in FBItTA and FBI mice, respectively; Fig. 3C). Thus, E-LTP was unaffected in FBItTA mice.

In contrast, L-LTP in FBItTA mice was markedly reduced as compared with the robust L-LTP observed in FBI mice (Fig. 3C). The slope of fEPSP 3–3.5 h and 5–5.5 h after tetanic stimulation in FBItTA mice was 148.6 ± 11.0% and 139.0 ± 10.2%, whereas that in FBI mice was 174.6 ± 10.2% and 167.6 ± 13.2%, respectively ($P < 0.05$). The fEPSPs elicited by stimulation of the second pathway to activate an independent set of Schaffer collaterals were unaltered throughout the experiment in both strains of mice. To clarify the biochemical effect of follistatin transgene expression, we analyzed the phosphorylation level of Smad 2/3 in the hippocampus of FBI and FBItTA. Phosphorylation of Smad 2/3 was significantly decreased in the hippocampus of FBItTA but not FBI (Supplemental Fig. S3). These results demonstrate that L-LTP was reduced in FBItTA mice, whose follistatin levels had an ability to suppress endogenous activin activity in the hippocampus.

Anxiety levels of ABItTA and FBItTA

Activin has multiple roles in the brain; for example, it influences anxiety-related behavior (Dow et al. 2005; Ageta et al. 2008; Zheng et al. 2008), modulates postnatal neurogenesis (Ageta et al. 2008), and protects neurons from ischemic damage (Tretter et al. 2000). In our previous study, we generated ACM4 and FSM transgenic mice in which activin and follistatin, respectively, were overexpressed in a forebrain-specific manner under the control of the αCaMKII promoter. FSM mice exhibited enhanced anxiety compared with wild-type littermates, while ACM4 mice showed reduced anxiety (Ageta et al. 2008). Therefore, we performed two behavioral analyses, such as a light and dark test and